



Original article

Sorafenib derivatives induce apoptosis through inhibition of STAT3 independent of Raf

Kuen-Feng Chen^{a,b,c,d,e}, Wei-Tien Tai^{a,b,c,d,e}, Jui-Wen Huang^f, Cheng-Yi Hsu^g, Wei-Lin Chen^g, Ann-Lii Cheng^{a,b,c,d,e}, Pei-Jer Chen^{a,b,c,d,e}, Chung-Wai Shiau^{g,*}

^a Department of Medical Research, National Taiwan University Hospital, 7, Chung-Shan South Road, Taipei, Taiwan, Republic of China

^b Department of Oncology, National Taiwan University Hospital, 7, Chung-Shan South Road, Taipei, Taiwan, Republic of China

^c Department of Internal Medicine, National Taiwan University Hospital, 7, Chung-Shan South Road, Taipei, Taiwan, Republic of China

^d Graduate Institute of Molecular Medicine, National Taiwan University College of Medicine, Taiwan

^e National Center of Excellence for Clinical Trial and Research, National Taiwan University Hospital, 7, Chung-Shan South Road, Taipei, Taiwan, Republic of China

^f Biomedical Engineering Research Laboratories, Industrial Technology Research Institute, 195, Sec. 4, Chung Hsing Rd., Chutung, Hsinchu, Taiwan

^g Institute of Biopharmaceutical Sciences, National Yang-Ming University, 155, Sec. 2, Linong Street, Taipei, Taiwan, Republic of China

ARTICLE INFO

Article history:

Received 15 September 2010

Received in revised form

24 March 2011

Accepted 3 April 2011

Available online 14 April 2011

Keywords:

Sorafenib

STAT3

Apoptosis

ABSTRACT

STAT3 is a transcription factor that modulates survival-directed transcription. It is persistently activated in many human cancers. Literature has shown that sorafenib, Raf kinase inhibitor, reduces Phospho-STAT3 and induces cell death. A series of sorafenib derivatives were synthesized as new inhibitors for STAT3. Urea, sulfonamide, and carboxamide linkers brought out different SARs from the end of sorafenib. Urea and carboxamide linked derivatives showed greater inhibition against STAT3 activity than sulfonamide linked derivatives. In particular, 1-(4-chloro-3-(trifluoromethyl)phenyl)-3-(4-(4-cyanophenoxy)phenyl)urea (**1**), a urea linker, was as potent as sorafenib in reducing P-STAT3 level and cell death but no inhibition for Raf activity. Such result provides a new lead for the design of STAT3 inhibitors.

© 2011 Elsevier Masson SAS. All rights reserved.

1. Introduction

Signal transducer and activator of transcription 3 (STAT3) is a transcription factor that regulates cell growth and survival by modulating the expression of target genes [1]. It acts as an oncogene which is constitutively active in many cancers including liver, lung, head and neck, prostate, and breast as well as myeloma and leukemia [2–6]. In a xenograft study, inhibition of STAT3 resulted in an increase in mouse survival. A key factor that regulates STAT3 activity is Src homology-2 containing protein tyrosine phosphatase-1 (SHP-1). From a mechanistic perspective, SHP-1 exhibits protein phosphatase activity which reduces the level of Phospho-STAT3 (P-STAT) and subsequently blocks the dimerization of P-STAT3. Therefore, expression of target genes, such as cyclin D1 and survivin transcribed by STAT3, is significantly reduced. In addition, extensive studies of SHP-1 protein and SHP-1 mRNA showed that expression level of SHP-1 was low in most cancer cells. Genetic increase in SHP-1 in cancer cells resulted in the suppression of cell growth,

suggesting that the SHP-1 gene acts as a tumor suppressor [7]. From the drug discovery point of view, development of a small molecule which can reduce P-STAT3 and increase SHP-1 level is a promising direction for cancer therapy.

A number of agents, including the natural products 5-hydroxy-2-methyl-1,4-naphthoquinone (a vitamin K3 analog), betulinic acid and boswellic acid have been reported to inhibit P-STAT3 level and reduces cell proliferation [8–13]. Although these agents show the ability to inhibit STAT3 activity, the dosage needed is higher than the clinical limitation. In addition, these natural products have the potential for off-target effects and activation or inactivation of other enzyme activity at high concentrations.

Sorafenib (BAY43-9006, Nexavar) is used clinically for renal carcinoma and hepatocellular carcinoma (HCC). It targets the c-Raf and b-Raf kinases and prolongs the survival of renal and HCC patients. Studies have shown that sorafenib was able to reduce the phosphorylation level of STAT3 in medulloblastoma and esophageal carcinoma [14,15]. Further study showed that sorafenib reduced P-STAT3 through activating SHP-1 phosphatase activity in HCC cells. To date, no correlation has been found between inhibition of Raf and activation of SHP-1 by the treatment with sorafenib.

* Corresponding author. Tel.: +886 2 28267930; fax: +886 2 28250883.

E-mail address: cwshiau@ym.edu.tw (C.-W. Shiau).

In addition, there are no reports showing that sorafenib derivatives inhibit STAT3 activity without affecting Raf activity.

In light of the ability of sorafenib to reduce the P-STAT3 level, here we synthesized novel sorafenib derivatives which retain the ability to reduce cell survival, but do not affect Raf kinase activity. We further provide evidence that these novel sorafenib derivatives mediate apoptosis through downregulation of P-STAT3 independent of Raf activity.

2. Chemistry

According to the X-ray structure of b-Raf and sorafenib, the amide group connected to the pyridine ring of sorafenib provides a hydrogen donor and forms a hydrogen bond with b-Raf in the ATP binding pocket [16]. The urea moiety of sorafenib also binds to the allosteric region by hydrogen bonding. To address the relationship between Raf kinase activity and downregulation of P-STAT3, we used a chemical approach to reduce the hydrogen bonding interaction between the amide group of sorafenib with Raf by replacing amide group with a phenylcyano group (Fig. 1). The Raf kinase activity of the resulting sorafenib analog **1** was tested by ELISA. To test the structure activity relationship of the downregulation of P-STAT3, we replaced the urea functional group in the sorafenib backbone with various amide and sulfonamide yielding compounds **2–11**. In addition, we replaced the pyridine ring with quinoline and used it as a platform to carry out structural modification, which generated a series of compounds **12–19** and **20–25**. These sorafenib derivatives were synthesized according to a general procedure described in Fig. 2. The inhibition of STAT3 and the Raf-1 activation by these compounds were tested by ELISA and western blot.

3. Biological evaluations

3.1. Development of sorafenib derivative lacking inhibition of Raf kinase activation

We synthesized a sorafenib derivative without providing hydrogen donor ability by replacing the pyridine ring and amide functional group with phenyl cyanide and exploring the ability of sorafenib and compound **1** to inhibit Raf kinase activity in PLC5 cells. Sorafenib was able to inhibit 50% of the Raf-1 kinase activity of the untreated cells in the PLC5 cells at 5 μ M (Fig. 3). In contrast, compound **1** treated cells showed the same Raf-1 activity as vehicle control.

3.2. Structure activity relationship of replacement of urea group and pyridine ring in cell death

The urea functional group linkage of sorafenib was replaced with various substitutes with sulfonylamide linkage, generating compounds **2–6** (Fig. 4). None of these derivatives within the electron donating or electron withdrawing group showed greater cell toxicity than sorafenib and compound **1**. Next, we changed the pyridine to a quinoline ring and amide linker to generate compounds

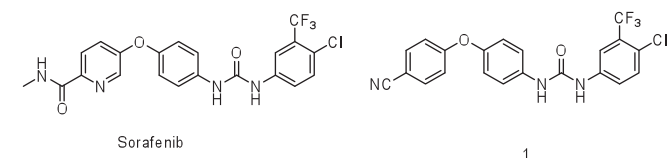
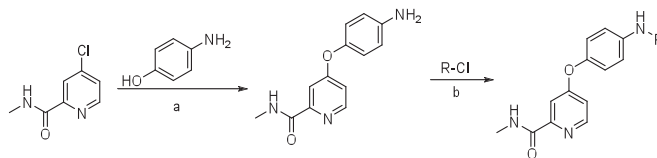
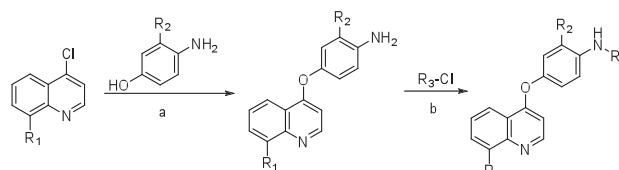


Fig. 1. Chemical structure of sorafenib and compound **1**.

Series A



Series B



Series C

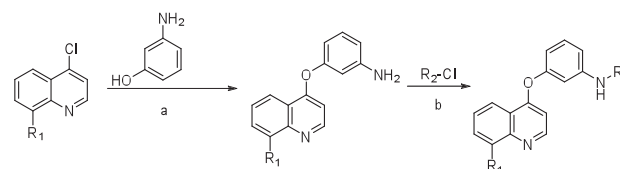


Fig. 2. General synthetic procedure for series A–C compounds: (a), K_2CO_3 , DMF; (b), pyridine, THF.

12–25. The amide linker showed different conformation from the sulfonyl linker, exhibiting better activity than sulfonyl linker compounds. For example, compound **16** showed a better cell toxicity than compound **12**. Compound **25** showed cytotoxicity comparable to sorafenib and **1**. We concluded that the urea and amide linkers exhibited the most potent cell toxicity in PLC5 cells.

3.3. Mechanistic validation of the mode of action of sorafenib derivatives

Previously, the sulfonyl linker and amide linker were shown to exhibit low activity against Raf kinase compared with sorafenib [17]. However, some of these compounds showed good

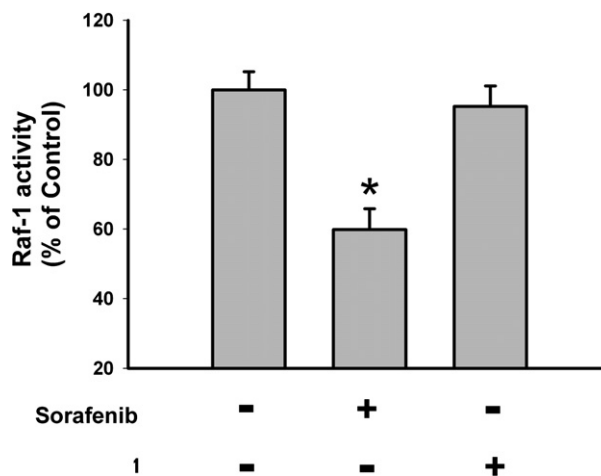
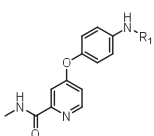
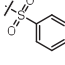
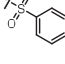
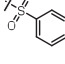
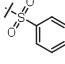
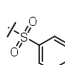


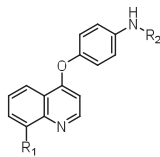
Fig. 3. Raf-1 activity of sorafenib and compound **1**. Huh-7 cells were exposed to sorafenib or compound **1** at 10 μ M for 24 h and cell lysates were analyzed for raf-1 activity. Columns, mean; bars, SD ($n = 3$). * $P < 0.05$.

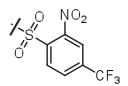
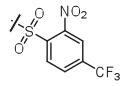
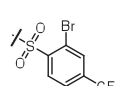
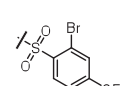
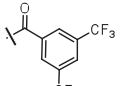
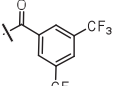
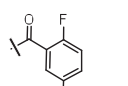
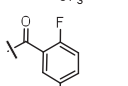
a



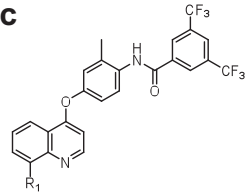
Cpd	R ₁	IC ₅₀ (μM) in PLC5 cells
Sorafenib		8.3
1		7.5
2		>40
3		>40
4		>40
5		>40
6		>40

b

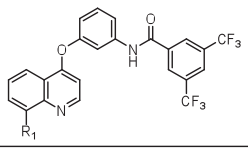


Cpd	R ₁	R ₂	IC ₅₀ (μM) in PLC5 cells
12	H		>40
13	NO ₂		>40
14	H		>40
15	NO ₂		>40
16	H		16.0
17	NO ₂		>40
18	H		21.1
19	NO ₂		>40

c



Cpd	R ₁	IC ₅₀ (μM) in PLC5 cells
20	NO ₂	>40
21	NH ₂	25.4
22	NHCOCH ₃	>40



Cpd	R ₁	IC ₅₀ (μM) in PLC5 cells
23	NO ₂	>40
24	NH ₂	19.0
25	NHCOCH ₃	10.8

Fig. 4. Chemical structure of compounds **2–25** and IC₅₀ of growth inhibition in PLC cells.

cytotoxicity in cancer cells. Therefore, we hypothesized that sorafenib derivatives downregulate P-STAT3 and enhance cell apoptosis. The sorafenib derivatives were tested for the inhibition of P-STAT3 by the ELISA. As shown in Fig. 5, sulfonyl linker compounds showed no appreciable change in P-STAT3. Compound **1** and some of the amide linker compounds showed a high degree of dephosphorylation of STAT3. The decreased level of P-STAT3 induced by these derivatives was correlated with cell toxicity. In the other words, these derivatives induced cell death in part through inhibition of STAT3. In addition, we also tested the downstream signal pathway after the inhibition of P-STAT3. Expression levels of the cyclin D1 and survivin, downstream target genes of STAT3, were assessed in compounds **1** and **12**. As shown in Fig. 6, compound **1** with STAT3 inhibitory activity, was able to reduce cyclin D1 and survivin level, but compound **12** had no effect on either protein. DNA fragmentation and flow cytometry analysis of PLC5 cells treated with compound **1** showed that cell death was attributed to the inhibition of STAT3 and further induced the apoptotic signal (Fig. 7).

4. Discussion

Recent data suggest that STAT3 serves as a key regulator of cell survival by activating its downstream survival signal pathway. This function is protective for chemotherapy cancer patients and renders STAT3 a good target for drug discovery. For example, a recent study demonstrated that cisplatin resistance in head and neck squamous cell carcinoma was associated with a high expression of STAT3 which played a role in the induction of reprogrammed survival pathways that circumvent cisplatin treatment [18]. Thus, this study focuses on the structural modification of sorafenib to develop a novel class of STAT3 inhibitors. Our premise that sorafenib inhibition of Raf and STAT3 could be structurally dissociated was borne out by compound **1**, which, devoid of Raf activity, exhibited the level of downregulation of P-STAT3 as sorafenib. Presumably, the cyanide group of compound **1** reduces its interaction with Raf. Subsequent modifications of sorafenib by changing the linker and pyridine ring to amide and quinoline (compounds **1**, **16**, and **25**, respectively) resulted in a decrease in STAT3-repressing potency.

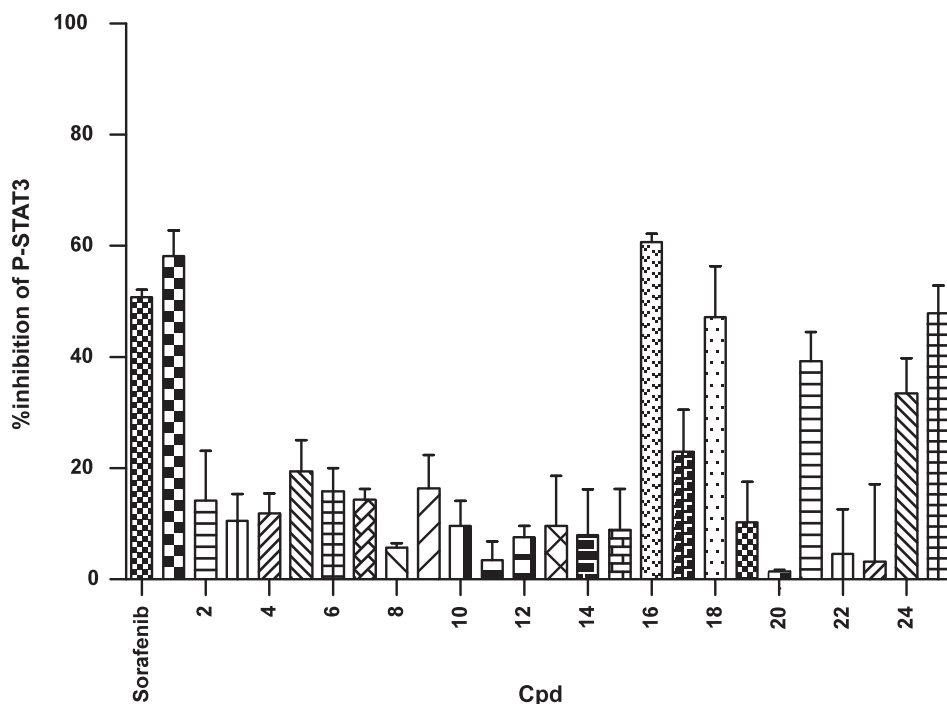


Fig. 5. Elisa analysis of the inhibitory effects of compounds **1–25** versus sorafenib, each at 10 μ M, on the IL-6 stimulated P-STAT in PLC5 cells after 24 h of treatment. Columns, mean, bars, SD ($N = 3$).

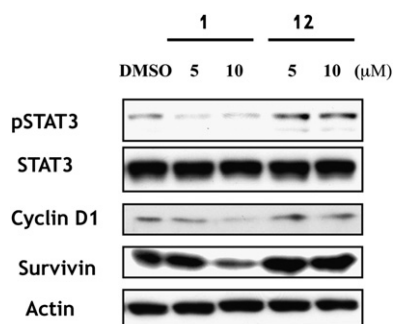


Fig. 6. Western blot analysis of the effect of compounds **1** and **12**, each at 5 μ M and 10 μ M on the phosphorylation of P-STAT3, STAT3, cyclin D and survivin in PLC5 cells in FBS-containing medium after 24 h of treatment.

5. Conclusion

We synthesized a series of sorafenib derivatives which showed the inhibition of STAT3 activity. In addition, these derivatives showed the cytotoxicity in HCC cells without reducing the Raf activity. Among these compounds, compound **1** demonstrated the potency as sorafenib in inhibition of P-STAT3 and cell growth. From a mechanistic study, compound **1** also showed the reduction expression of survivin and cyclin D1 after blocking the STAT3 signaling cascade. In addition, it provides a useful pharmacological tool with which to study therapeutic relevance in the treatment of HCC with dysregulated STAT3 expression and drug resistance. Thus, these data give the potential use of this anti-STAT3 agent in the treatment of HCC. Testing of compound **1** in an in vivo HCC model is currently being pursued.

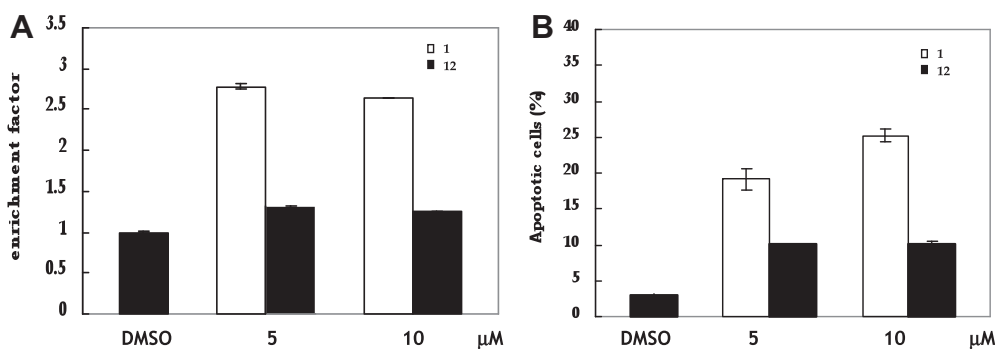


Fig. 7. (A). Elisa analysis of cell death induced by compound **1** and **12**, at 5, and 10 μ M, after 24 h of treatment in PLC5 cells (B). Flow cytometry analysis of cell death induced by compound **1** and **12**, at 5, and 10 μ M, after 24 h of treatment in PLC5 cells.

6. Experimental section

6.1. Material

Proton nuclear magnetic resonance (^1H NMR) spectra were recorded on Bruker DPX300 (400 MHz) instruments. Chemical shifts are reported in ppm. Peak multiplicities are expressed as follows: s, singlet; d, doublet; t, triplet; q, quartet; dd, doublet of doublet; ddd, doublet of doublet of doublets; dt, doublet of triplet; brs, broad singlet; m, multiplet. Coupling constants (J values) are given in hertz (Hz). Reaction progress was determined by thin layer chromatography (TLC) analysis on silica gel 60 F254 plate (Merck). Chromatographic purification was carried on silica gel columns 60 (0.063–0.200 mm or 0.040–0.063 mm, Merck), basic silica gel. Commercial reagents and solvents were used without additional purification. Abbreviations are used as follows: CDCl_3 , deuterated chloroform; DMSO- d_6 , dimethyl sulfoxide- d_6 ; EtOAc, ethyl acetate; DMF, N,N -dimethylformamide; MeOH, methanol; THF, tetrahydrofuran; EtOH, ethanol; DMSO, dimethyl sulfoxide; NMP, N -methylpyrrolidone. High resolution mass spectra were recorded on a FINNIGAN MAT 95S mass spectrometer.

6.2. Chemical synthesis

6.2.1. Procedures for compound 1

To a 50 mL THF solution of triphosgen (0.30 g, 1.0 mmol), 4-chloro-3-(trifluoromethyl)aniline (0.21 g, 1.1 mmol) and 2 equivalent of triethyl amine were added. The mixture was heated to 50 °C for 30 min. After the temperature was back to room temperature, 4-(4-aminophenoxy)benzonitrile in the 10 mL THF solution was added to the mixture and heated to 50 °C for another 30 min. The mixture was evaporated, diluted with water and extracted with EtOAc. The extract was washed with brine, dried over anhydrous magnesium sulfate, and concentrated under reduced pressure to give **1** (0.34 g, 80%).

6.2.1.1. 1-(4-Chloro-3-(trifluoromethyl)phenyl)-3-(4-(4-cyanophenoxy)phenyl)urea (1). ^1H NMR (400 MHz, CDCl_3): δ 9.17 (s, 1H), 8.94 (s, 1H), 8.10 (s, 1H), 7.81 (d, 2H, $J = 6.8$), 7.63–7.59 (m, 2H), 7.54 (d, 2H, $J = 7.2$ Hz), 7.10 (d, 2H, $J = 6.8$ Hz), 7.05 (d, 2H, $J = 7.2$ Hz); ^{13}C NMR (100 MHz, methanol- d_4): δ 163.7, 163.6, 154.8, 151.4, 151.2, 140.1, 137.7, 137.4, 135.3, 132.9, 129.7, 129.4, 129.1, 128.8, 128.3, 125.6, 125.5, 125.4, 124.2, 122.9, 122.4, 122.3, 122.1, 120.2, 119.7, 118.8, 118.7, 118.6, 118.6, 106.5, 106.4; HRMS calculated for $\text{C}_{21}\text{H}_{13}\text{ClF}_3\text{N}_3\text{O}_2$ ($M + \text{H}$): 431.0648. Found: 431.0656.

6.2.2. General procedures for the synthesis of compounds 2–25

In a 25 mL two-necked round flask, aniline derivatives (1 mmol) and catalytic amount of pyridine were placed in anhydrous THF (10 mL) at room temperature. Acyl chloride or sulfonyl chloride compounds were added to the mixture and stirred for 2 h at room temperature. The solvent was removed under vacuum and the crude residue purified by chromatography on a silica gel column using EtOAc/Hexane as eluent (1/10 to 1/2). This procedure afforded the expected coupling product as a white solid from 70% to 95% yield.

6.2.2.1. *N*-methyl-4-(4-(phenylsulfonamido)phenoxy)picolinamide (2). ^1H NMR (400 MHz, CDCl_3): δ 8.36 (d, 1H, $J = 5.6$ Hz), 8.01 (brs, 1H), 7.76 (d, 2H, $J = 7.6$ Hz), 7.59 (s, 1H), 7.54 (t, 1H, $J = 8.0$ Hz), 7.46 (t, 2H, $J = 8.0$ Hz), 7.12 (d, 2H, $J = 8.8$ Hz), 6.94 (d, 2H, $J = 8.8$ Hz), 6.92–6.90 (m, 1H), 3.00 (d, 3H, $J = 5.2$ Hz); ^{13}C NMR (100 MHz, CDCl_3): δ 166.0, 164.6, 152.1, 151.0, 149.7, 138.9, 134.2, 133.0, 129.0, 127.1, 123.9, 121.6, 114.3, 109.9, 26.1; HRMS calculated for $\text{C}_{19}\text{H}_{17}\text{N}_3\text{O}_4\text{S}$ ($M + \text{H}$): 383.0940. Found: 383.0941.

6.2.2.2. *N*-methyl-4-(4-(4-nitrophenylsulfonamido)phenoxy)picolinamide (3). ^1H NMR (400 MHz, CDCl_3): δ 8.39 (d, 1H, $J = 5.6$ Hz), 8.30 (d, 2H, $J = 8.8$ Hz), 8.07 (brs, 1H), 7.93 (d, 2H, $J = 8.8$ Hz), 7.49 (s, 1H), 7.17 (d, 2H, $J = 8.8$ Hz), 7.01–6.98 (m, 3H), 3.00 (d, 3H, $J = 5.2$ Hz); HRMS calculated for $\text{C}_{19}\text{H}_{16}\text{N}_4\text{O}_6\text{S}$ ($M + \text{H}$): 428.0791. Found: 428.0798.

6.2.2.3. 4-(4-(4-Fluorophenylsulfonamido)phenoxy)-*N*-methylpicolinamide (4). ^1H NMR (400 MHz, CDCl_3): δ 8.37 (d, 1H, $J = 5.6$ Hz), 8.00 (brs, 1H), 7.77–7.43 (m, 2H), 7.57 (s, 1H), 7.17–7.09 (m, 4H), 6.99–6.93 (m, 4H), 3.00 (d, 3H, $J = 4.8$ Hz); NMR (100 MHz, CDCl_3): δ 166.5, 165.9, 164.6, 163.9, 152.1, 151.2, 149.7, 135.0, 134.0, 130.0, 129.9, 124.1, 121.7, 116.4, 116.2, 114.5, 109.8, 26.19; HRMS calculated for $\text{C}_{19}\text{H}_{16}\text{FN}_3\text{O}_4\text{S}$ ($M + \text{H}$): 401.0846. Found: 401.0849.

6.2.2.4. 4-(4-(4-*tert*-Butylphenylsulfonamido)phenoxy)-*N*-methylpicolinamide (5). ^1H NMR (400 MHz, CDCl_3): δ 8.33 (d, 1H, $J = 6.0$ Hz), 8.21 (brs, 1H), 7.79 (brs, 1H), 7.69 (d, 2H, $J = 6.8$ Hz), 7.62 (s, 1H), 7.44 (d, 2H, $J = 6.8$ Hz), 7.15 (d, 2H, $J = 6.8$ Hz), 6.91 (s, 2H, $J = 6.8$ Hz), 6.88–6.86 (m, 1H), 2.98 (d, 3H, $J = 5.2$ Hz); ^{13}C NMR (100 MHz, CDCl_3): δ 166.0, 164.6, 156.8, 152.2, 150.8, 149.7, 136.1, 134.4, 127.0, 126.1, 123.6, 121.6, 114.1, 110.1, 35.1, 30.1, 26.1; HRMS calculated for $\text{C}_{23}\text{H}_{25}\text{N}_3\text{O}_4\text{S}$ ($M + \text{H}$): 439.1566. Found: 439.1564.

6.2.2.5. *N*-methyl-4-(4-(naphthalene-2-sulfonamido)phenoxy)picolinamide (6). ^1H NMR (400 MHz, CDCl_3): δ 8.34 (s, 1H), 8.30 (d, 1H, $J = 5.2$ Hz), 8.05–8.02 (m, 1H), 7.89–7.83 (m, 4H), 7.74 (dd, 1H, $J = 8.4$, 1.6 Hz), 7.60–7.52 (m, 3H), 7.16 (d, 2H, $J = 8.8$ Hz), 6.88 (d, 2H, $J = 8.8$ Hz), 6.84–6.82 (m, 1H); ^{13}C NMR (100 MHz, CDCl_3): 165.9, 164.6, 152.1, 151.0, 149.7, 135.9, 134.9, 134.2, 132.0, 129.4, 129.3, 128.9, 128.7, 127.9, 127.5, 123.9, 122.2, 121.6, 114.2, 110.1, 26.2; HRMS calculated for $\text{C}_{23}\text{H}_{19}\text{N}_3\text{O}_4\text{S}$ ($M + \text{H}$): 433.1096. Found: 433.1079.

6.2.2.6. 4-(4-(2-Bromo-4-(trifluoromethyl)phenylsulfonamido)phenoxy)-*N*-methylpicolinamide (7). ^1H NMR (400 MHz, CDCl_3): δ 8.35 (d, 1H, $J = 5.6$ Hz), 8.15 (d, 1H, $J = 8.0$ Hz), 7.79 (brs, 1H), 7.96 (s, 1H), 7.67 (d, 2H, $J = 8.0$ Hz), 7.57 (s, 1H), 7.18 (d, 2H, $J = 9.2$ Hz), 6.95 (d, 2H, $J = 9.2$ Hz), 6.90–6.88 (m, 1H), 2.98 (d, 3H, $J = 5.2$ Hz); ^{13}C NMR (100 MHz, CDCl_3): δ 165.7, 164.5, 152.2, 151.6, 149.8, 141.5, 136.1, 135.8, 135.5, 135.2, 132.7, 132.2 (m), 124.9 (m), 124.1, 123.5, 121.7, 120.8, 120.4, 114.5, 110.0, 26.1; HRMS calculated for $\text{C}_{20}\text{H}_{15}\text{BrF}_3\text{N}_3\text{O}_4\text{S}$ ($M + \text{H}$): 528.9919. Found: 528.9917.

6.2.2.7. *N*-methyl-4-(4-(2-nitrophenylsulfonamido)phenoxy)picolinamide (8). ^1H NMR (400 MHz, CDCl_3): δ 8.37 (d, 1H, $J = 6.0$ Hz), 7.98 (brs, 1H), 7.86–7.83 (m, 2H), 7.72–7.68 (m, 2H), 7.55 (s, 1H), 7.24 (d, 2H, $J = 8.8$ Hz), 6.98 (d, 2H, $J = 8.8$ Hz), 6.94–6.92 (m, 1H), 2.98 (d, 3H, $J = 4.8$ Hz); HRMS calculated for $\text{C}_{19}\text{H}_{16}\text{N}_4\text{O}_6\text{S}$ ($M + \text{H}$): 428.0791. Found: 428.0796.

6.2.2.8. 4-(4-(3,5-Bis(trifluoromethyl)benzamido)phenoxy)-*N*-methylpicolinamide (9). ^1H NMR (400 MHz, CDCl_3): δ 9.92 (s, 1H), 8.40 (s, 1H), 8.33 (d, 1H, $J = 5.6$ Hz), 8.10 (q, 1H, $J = 5.2$ Hz), 7.90 (s, 1H), 7.71 (d, 2H, $J = 8.8$ Hz), 7.40 (d, 1H, $J = 2.8$ Hz), 6.99–6.97 (m, 1H), 6.93 (d, 2H, $J = 8.8$ Hz), 2.91 (d, 3H, $J = 4.8$ Hz); ^{13}C NMR (100 MHz, methanol- d_4): δ 167.8, 166.8, 165.1, 153.4, 151.8, 151.6, 138.6, 137.6, 133.6, 133.3, 133.0, 132.6, 129.4 (d), 126.2 (m), 126.0, 124.2, 123.2, 122.4, 115.2, 110.7, 26.4; HRMS calculated for $\text{C}_{22}\text{H}_{15}\text{F}_6\text{N}_3\text{O}_3$ ($M + \text{H}$): 483.1018. Found: 483.1017.

6.2.2.9. 4-(4-(5-Fluoro-2-(trifluoromethyl)benzamido)phenoxy)-*N*-methylpicolinamide (10). ^1H NMR (400 MHz, CDCl_3): δ 8.66 (d, 1H, $J = 12.4$ Hz), 8.31–8.26 (m, 2H), 7.93 (s, 1H), 7.70–7.65 (m, 3H), 7.56 (t, 1H, $J = 2.4$ Hz), 7.24–7.19 (m, 1H), 7.02 (d, 2H, $J = 6.4$ Hz), 6.89–6.87 (m, 1H), 2.90 (d, 3H, $J = 3.2$ Hz); ^{13}C NMR (100 MHz, methanol- d_4):

δ 166.2, 164.5, 162.9, 160.4, 160.0, 159.9, 152.2, 150.4, 149.7, 135.0, 130.6 (m), 129.8 (m), 128.3, 128.1, 127.7, 127.4, 124.5, 122.5, 122.4, 122.3, 121.8, 121.5, 117.2, 117.0, 114.1, 110.1, 26.1; HRMS calculated for $C_{21}H_{15}F_4N_3O_3$ (M + H): 433.1050. Found: 433.0152.

6.2.2.10. *N*-methyl-4-(4-(trifluoromethyl)benzamido)phenoxy)picolinamide (**11**). 1H NMR (400 MHz, $CDCl_3$): δ 9.45 (s, 1H), 8.31 (d, 1H, J = 5.6 Hz), 8.15 (s, 1H), 8.08 (d, 2H, J = 8.0 Hz), 7.71–7.65 (m, 3H), 7.50 (d, 1H, J = 2.4 Hz), 7.47 (t, 1H, J = 8.0 Hz), 6.96–6.91 (m, 3H), 2.92 (d, 3H, J = 5.2 Hz); ^{13}C NMR (100 MHz, $CDCl_3$): δ 166.4, 164.8, 164.7, 151.8, 149.9149.8, 138.8, 135.5, 131.4, 131.1, 130.8, 130.7, 130.5, 129.1, 128.1, 125.0, 124.3 (m), 122.6, 122.3, 121.2, 114.4, 109.5, 26.1; HRMS calculated for $C_{21}H_{16}F_3N_3O_3$ (M + H): 415.1144. Found: 415.1146.

6.2.2.11. 2-Nitro-*N*-(4-(quinolin-4-yloxy)phenyl)-4-(trifluoromethyl)benzenesulfonamide (**12**). 1H NMR (400 MHz, $CDCl_3$): δ 8.71 (d, 1H, J = 5.2 Hz), 8.28 (d, 1H, J = 8.4 Hz), 8.12 (d, 1H, J = 8.4 Hz), 8.10 (s, 1H), 8.05 (d, 1H, J = 8.4 Hz), 7.89 (d, 1H, J = 8.4 Hz), 7.80–7.76 (m, 1H), 7.61–7.57 (m, 1H), 7.31 (d, 2H, J = 8.8 Hz), 7.13 (d, 1H, J = 8.8 Hz), 6.53 (d, 1H, J = 5.2 Hz); HRMS calculated for $C_{22}H_{14}F_3N_3O_5S$ (M + H): 489.0606. Found: 489.0610.

6.2.2.12. 2-Nitro-*N*-(4-(8-nitroquinolin-4-yloxy)phenyl)-4-(trifluoromethyl)benzenesulfonamide (**13**). 1H NMR (400 MHz, $CDCl_3$): δ 8.78 (d, 1H, J = 5.2 Hz), 8.51 (d, 1H, J = 8.8 Hz), 8.19 (s, 1H), 8.12–8.02 (m, 3H), 7.89 (t, 1H, J = 9.6 Hz), 7.62 (t, 1H, J = 8.4 Hz), 7.34 (d, 2H, J = 9.6 Hz), 7.15 (d, 2H, J = 9.6 Hz), 6.91 (d, 1H, J = 6.8 Hz), 6.59 (d, 1H, J = 5.2 Hz), 6.55 (d, 1H, J = 6.8 Hz); HRMS calculated for $C_{22}H_{13}F_3N_4O_7S$ (M + H): 534.0457. Found: 534.0423.

6.2.2.13. 2-Bromo-*N*-(4-(quinolin-4-yloxy)phenyl)-4-(trifluoromethyl)benzenesulfonamide (**14**). 1H NMR (400 MHz, $CDCl_3$): δ 8.65 (d, 1H, J = 5.2 Hz), 8.25 (d, 1H, J = 8.4 Hz), 8.18 (d, 1H, J = 8.4 Hz), 8.07 (d, 1H, J = 8.4 Hz), 7.98 (s, 1H), 7.73 (t, 1H, J = 7.6 Hz), 7.67 (d, 1H, J = 8.4 Hz), 7.54 (t, 1H, J = 7.6 Hz), 7.24 (d, 2H, J = 8.8 Hz), 7.05 (d, 2H, J = 8.8 Hz), 6.43 (d, 1H, J = 5.2 Hz); ^{13}C NMR (100 MHz, $CDCl_3$): δ 161.3, 152.6, 150.9, 149.7, 141.4, 135.9, 135.6, 135.3, 132.7, 132.4, 132.2 (m), 130.3, 129.1, 126.3, 124.9 (m), 124.4, 123.5, 122.1, 122.0, 121.9, 121.6, 121.3, 120.8, 120.4, 116.3, 104.4; HRMS calculated for $C_{22}H_{14}BrF_3N_2O_3S$ (M + H): 521.9861. Found: 521.9858.

6.2.2.14. 2-Bromo-*N*-(4-(8-nitroquinolin-4-yloxy)phenyl)-4-(trifluoromethyl)benzenesulfonamide (**15**). 1H NMR (400 MHz, $CDCl_3$): δ 8.76 (d, 1H, J = 5.2 Hz), 8.49 (d, 1H, J = 8.4 Hz), 8.18 (d, 1H, J = 8.4 Hz), 8.04 (d, 1H, J = 7.6 Hz), 7.99 (s, 1H), 7.68 (d, 1H, J = 8.4 Hz), 7.60 (t, 1H, J = 8.4 Hz), 7.25 (d, 2H, J = 8.4 Hz), 7.07 (d, 2H, J = 8.4 Hz), 6.53 (d, 1H, J = 5.2 Hz); HRMS calculated for $C_{22}H_{13}BrF_3N_3O_5S$ (M + H): 566.9711. Found: 566.9706.

6.2.2.15. *N*-(4-(quinolin-4-yloxy)phenyl)-3,5-bis(trifluoromethyl)benzamide (**16**). 1H NMR (400 MHz, $CDCl_3$): δ 10.02 (s, 1H), 8.59 (d, 1H, J = 5.6 Hz), 8.37 (s, 2H), 8.34 (d, 1H, J = 8.4 Hz), 7.99 (d, 1H, J = 8.4 Hz), 7.92 (s, 1H), 7.80 (d, 2H, J = 9.2 Hz), 7.70 (t, 1H, J = 7.6 Hz), 6.56 (t, 1H, J = 7.6 Hz), 7.14 (d, 2H, J = 9.2 Hz), 6.52 (d, 1H, J = 5.2 Hz); ^{13}C NMR (100 MHz, $DMSO-d_6$): δ 162.6, 161.0, 151.5, 150.0, 149.2, 137.0, 136.1, 131.0, 130.7, 130.4, 130.3, 130.0, 128.8, 128.5 (m), 126.4, 125.2 (m), 124.5, 122.5, 121.7, 121.5, 121.3, 120.6, 104.3; HRMS calculated for $C_{24}H_{14}F_6N_2O_2$ (M + H): 476.0959. Found: 476.0958.

6.2.2.16. *N*-(4-(8-nitroquinolin-4-yloxy)phenyl)-3,5-bis(trifluoromethyl)benzamide (**17**). 1H NMR (400 MHz, $CDCl_3$): δ 9.05 (s, 1H), 8.69 (d, 1H, J = 5.0 Hz), 8.59 (d, 1H, J = 5.0 Hz), 8.35 (s, 2H), 8.06 (d, 1H, J = 7.8 Hz), 7.97 (s, 1H), 7.80 (d, 2H, J = 9.0 Hz), 7.63 (t, 1H, J = 8.6 Hz),

7.16 (d, 2H, J = 9.0 Hz), 6.62 (d, 1H, J = 5.0 Hz); HRMS calculated for $C_{24}H_{13}F_6N_3O_4$ (M + H): 521.0810. Found: 521.0814.

6.2.2.17. 2-Fluoro-*N*-(4-(quinolin-4-yloxy)phenyl)-5-(trifluoromethyl)benzamide (**18**). 1H NMR (400 MHz, $CDCl_3$): δ 8.83 (d, 1H, J = 12.8 Hz), 8.68 (d, 1H, J = 5.2 Hz), 8.39–8.30 (m, 2H), 8.11 (d, 1H, J = 8.4 Hz), 7.79–7.67 (m, 4H), 7.58 (t, 1H, J = 8.0 Hz), 7.27–7.22 (m, 1H), 7.18 (d, 2H, J = 9.2 Hz), 6.56 (d, 1H, J = 5.2 Hz); ^{13}C NMR (100 MHz, methanol- d_4): δ 164.4, 164.2, 163.8, 161.7, 151.9, 151.8, 149.7, 137.5, 132.1 (m), 131.2 (m), 128.9 (m), 128.3, 128.1, 127.9, 126.5, 126.3, 123.7, 123.6, 123.0, 122.7, 122.6, 119.1, 119.8, 118.7, 118.5, 105.2; HRMS calculated for $C_{23}H_{14}F_4N_2O_2$ (M + H): 426.0991. Found: 426.0991.

6.2.2.18. 2-Fluoro-*N*-(4-(8-nitroquinolin-4-yloxy)phenyl)-5-(trifluoromethyl)benzamide (**19**). 1H NMR (400 MHz, $CDCl_3$): δ 8.81 (d, 1H, J = 5.2 Hz), 8.59 (d, 1H, J = 8.8 Hz), 8.53–8.47 (m, 2H), 8.06 (d, 1H, J = 7.6 Hz), 7.83–7.77 (m, 3H), 7.64 (t, 1H, J = 7.6 Hz), 7.37–7.32 (m, 1H), 7.23–7.20 (m, 2H), 6.68 (d, 1H, J = 5.2 Hz); HRMS calculated for $C_{23}H_{13}F_4N_3O_4$ (M + H): 471.0842. Found: 471.0850.

6.2.2.19. *N*-(2-methyl-4-(8-nitroquinolin-4-yloxy)phenyl)-3,5-bis(trifluoromethyl)benzamide (**20**). 1H NMR (400 MHz, $CDCl_3$): δ 9.86 (s, 1H), 8.45 (d, 1H, J = 5.2 Hz), 8.38 (s, 2H), 8.31 (d, 1H, J = 8.4 Hz), 7.92 (s, 1H), 7.89 (d, 1H, J = 8.4 Hz), 7.69–7.63 (m, 2H), 7.53 (t, 1H, J = 7.6 Hz), 7.33 (s, 1H), 7.28 (d, 1H, J = 8.4 Hz), 6.33 (d, 1H, J = 5.2 Hz); HRMS calculated for $C_{25}H_{15}F_6N_3O_4$ (M + H): 535.0967. Found: 535.0956.

6.2.2.20. *N*-(4-(8-aminoquinolin-4-yloxy)-2-methylphenyl)-3,5-bis(trifluoromethyl)benzamide (**21**). 1H NMR (400 MHz, $CDCl_3$): δ 8.49 (d, 1H, J = 2.0 Hz), 8.27 (s, 1H), 8.02 (s, 1H), 7.94 (s, 1H), 7.65 (d, 1H, J = 8.0 Hz), 7.48–7.45 (m, 2H), 7.37–7.32 (m, 2H), 6.96 (d, 1H, J = 7.6 Hz), 4.95 (s, 2H), 2.16 (s, 3H); HRMS calculated for $C_{25}H_{17}F_6N_3O_2$ (M + H): 505.1225. Found: 505.1216.

6.2.2.21. *N*-(4-(8-acetamidoquinolin-4-yloxy)-2-methylphenyl)-3,5-bis(trifluoromethyl)benzamide (**22**). 1H NMR (400 MHz, $CDCl_3$): δ 9.77 (s, 1H), 9.36 (s, 1H), 8.65 (d, 1H, J = 7.2 Hz), 8.46 (s, 2H), 8.44 (d, 1H, J = 5.2 Hz), 7.97 (s, 1H), 7.87 (d, 1H, J = 8.4 Hz), 7.72 (d, 1H, J = 8.4 Hz), 7.50 (d, 1H, J = 2.0 Hz), 7.37 (t, 1H, J = 8.0 Hz), 7.28 (d, 1H, J = 8.4 Hz), 6.41 (d, 1H, J = 5.2 Hz), 2.26 (s, 3H), 2.10 (s, 3H); ^{13}C NMR (100 MHz, $CDCl_3$): δ 169.2, 163.0, 161.2, 152.0, 148.8, 139.5, 137.2, 136.7, 133.8, 132.6, 132.3, 132.2, 132.0, 131.6, 127.8, 127.1, 126.3, 125.2 (m), 124.2, 121.5, 120.4, 118.8, 118.3, 116.7, 115.7, 113.8, 25.0, 15.4; HRMS calculated for $C_{27}H_{19}F_6N_3O_3$ (M + H): 547.1331. Found: 547.1325.

6.2.2.22. *N*-(3-(8-nitroquinolin-4-yloxy)phenyl)-3,5-bis(trifluoromethyl)benzamide (**23**). 1H NMR (400 MHz, $CDCl_3$): δ 8.78 (d, 1H, J = 5.6 Hz), 8.58 (d, 1H, J = 8.4 Hz), 8.52 (s, 1H), 8.31 (s, 2H), 8.22 (s, 1H), 8.08–8.04 (m, 2H), 7.71 (s, 1H), 7.64 (t, 1H, J = 8.0 Hz), 7.53–7.49 (m, 2H), 7.03 (d, 1H, J = 7.2 Hz), 6.71 (d, 1H, J = 4.8 Hz); HRMS calculated for $C_{24}H_{13}F_6N_3O_4$ (M + H): 521.0810. Found: 521.0821.

6.2.2.23. *N*-(3-(8-aminoquinolin-4-yloxy)phenyl)-3,5-bis(trifluoromethyl)benzamide (**24**). 1H NMR (400 MHz, $CDCl_3$): δ 8.55 (d, 1H, J = 4.8 Hz), 8.29 (s, 2H), 8.05 (s, 1H), 7.90 (s, 1H), 7.60 (d, 1H, J = 8.4 Hz), 7.55 (s, 1H), 7.70–7.43 (m, 2H), 7.34 (t, 1H, J = 8.0 Hz), 7.01 (d, 1H, J = 8.0 Hz), 6.96 (d, 1H, J = 7.9 Hz), 6.63 (d, 1H, J = 4.8 Hz); ^{13}C NMR (100 MHz, $CDCl_3$): δ 163.1, 161.3, 155.3, 147.9, 143.6, 139.9, 138.8, 136.5, 132.7, 132.4, 131.7, 130.6, 127.5 (d), 127.0, 126.8, 125.3 (m), 124.1, 122.0, 118.7, 117.4, 117.2, 113.1, 111.1, 110.0, 105.4; HRMS calculated for $C_{24}H_{15}F_6N_3O_2$ (M + H): 491.1068. Found: 491.1068.

6.2.2.24. *N*-(3-(8-acetamidoquinolin-4-yloxy)phenyl)-3,5-bis(trifluoromethyl)benzamide (**25**). ^1H NMR (400 MHz, CDCl_3): δ 9.77 (s, 1H), 8.74 (d, 1H, $J = 7.6$ Hz), 8.54 (d, 1H, $J = 5.2$ Hz), 8.48 (s, 1H), 8.39 (s, 2H), 8.04 (s, 1H), 7.87 (d, 1H, $J = 8.4$ Hz), 7.67–7.60 (m, 2H), 7.50–7.43 (m, 2H), 7.37 (t, 1H, $J = 8.0$ Hz), 7.00 (d, 1H, $J = 8.4$ Hz), 6.65 (d, 1H, $J = 5.2$ Hz), 2.30 (s, 3H); ^{13}C NMR (100 MHz, CDCl_3): δ 169.3, 163.1, 161.7, 154.6, 148.7, 139.6, 136.6, 133.8, 132.7, 132.4, 132.1, 131.7, 130.8, 127.8 (d), 126.9, 126.5, 125.3 (m), 124.2, 121.5, 120.8, 117.7, 117.3, 116.8, 115.7, 113.2, 104.9, 25.0; HRMS calculated for $\text{C}_{26}\text{H}_{17}\text{F}_6\text{N}_3\text{O}_3$ ($M + H$): 533.1174. Found: 533.1167.

6.3. Biological assay

6.3.1. Cell culture

The PLC/PRF/5 (PLC5), Sk-Hep-1, Hep3B and Cells were maintained in DMEM supplemented with 10% FBS, 100 units/mL penicillin G, 100 $\mu\text{g}/\text{mL}$ streptomycin sulfate and 25 $\mu\text{g}/\text{mL}$ amphotericin B in a 37 °C humidified incubator in an atmosphere of 5% CO_2 in air.

6.3.2. Phospho-STAT3-level

A PathScan Phospho-Stat3 (Tyr705) Sandwich ELISA Kit was used for the detection of phospho-STAT3 (Cell Signaling, Danvers, MA). PLC5 cells were pre-treated with IL-6 1 ng/mL and then exposed with various compounds at 10 μM for 24 h. After incubation with cell lysates, both non-phospho- and phospho-Stat3 proteins are captured by the coated antibody. The expression of phospho-STAT3 was measured at 450 nm absorbance.

6.3.3. Western blot

PLC5 cells were treated with compound 1 and 12 at 5 and 10 μM for 24 h. Cell lysates were analyzed by western blot.

6.3.4. Cell death detection ELISA

The effect of compound 1 and 12 on cell viability was assessed cell death ELISA assay (Roche Applied Science, Mannheim, Germany). PLC5 cells were treated with Compound 1 and 12 at 5 and 10 μM for 24 h. The cells were collected and applied to the standard protocol provided by manufacture.

6.3.5. Apoptosis analysis

The measurement of apoptotic cells by flow cytometry (sub-G1). After Compound 1 and 12 treatment, cells were trypsinized, collected by centrifugation and resuspended in PBS. After centrifugation, the cells were washed in PBS and resuspended in potassium iodide (PI) staining solution. Specimens were incubated in the dark for 30 min at 37 °C and then analyzed with an EPICS Profile II flow cytometer (Coulter Corp., Hialeah, FL). All experiments were performed in triplicate.

Acknowledgments

We thank the National Science Council, Taiwan (NSC98-2320-B-010-005-My3) and National Yang Ming University, Taiwan for

financial support. C.W. S. also thanks the National Research Institute of Chinese Medicine for NMR support.

References

- [1] J.F. Bromberg, M.H. Wrzeszczynska, G. Devgan, Y. Zhao, R.G. Pestell, C. Albanese, J.E. Darnell Jr., Stat3 as an oncogene, *Cell* 98 (1999) 295–303.
- [2] M. Kortylewski, M. Kujawski, T. Wang, S. Wei, S. Zhang, S. Pilon-Thomas, G. Niu, H. Kay, J. Mule, W.G. Kerr, R. Jove, D. Pardoll, H. Yu, Inhibiting Stat3 signaling in the hematopoietic system elicits multicomponent antitumor immunity, *Nat. Med.* 11 (2005) 1314–1321.
- [3] S. Dong, S.J. Chen, D.J. Twardy, Cross-talk between retinoic acid and STAT3 signaling pathways in acute promyelocytic leukemia, *Leuk. Lymphoma* 44 (2003) 2023–2029.
- [4] Q. Lin, R. Lai, L.R. Chirieac, C. Li, V.A. Thomazy, I. Grammatikakis, G.Z. Rassidakis, W. Zhang, Y. Fujio, K. Kunisada, S.R. Hamilton, H.M. Amin, Constitutive activation of JAK3/STAT3 in colon carcinoma tumors and cell lines: inhibition of JAK3/STAT3 signaling induces apoptosis and cell cycle arrest of colon carcinoma cells, *Am. J. Pathol.* 167 (2005) 969–980.
- [5] M.S. Redell, D.J. Twardy, Targeting transcription factors for cancer therapy, *Curr. Pharm. Des.* 11 (2005) 2873–2887.
- [6] J. Turkson, R. Jove, STAT proteins: novel molecular targets for cancer drug discovery, *Oncogene* 19 (2000) 6613–6626.
- [7] C. Wu, M. Sun, L. Liu, G.W. Zhou, The function of the protein tyrosine phosphatase SHP-1 in cancer, *Gene* 306 (2003) 1–12.
- [8] A.B. Kunnumakkara, A.S. Nair, B. Sung, M.K. Pandey, B.B. Aggarwal, Boswellic acid blocks signal transducers and activators of transcription 3 signaling, proliferation, and survival of multiple myeloma via the protein tyrosine phosphatase SHP-1, *Mol. Cancer Res.* 7 (2009) 118–128.
- [9] M.K. Pandey, B. Sung, B.B. Aggarwal, Butein suppresses STAT3 activation pathway through induction of protein tyrosine phosphatase SHP-1 in human multiple myeloma cells, *Int. J. Cancer* 127 (2010) 282–292.
- [10] M.K. Pandey, B. Sung, K.S. Ahn, B.B. Aggarwal, Butein suppresses constitutive and inducible signal transducer and activator of transcription (STAT) 3 activation and STAT3-regulated gene products through the induction of a protein tyrosine phosphatase SHP-1, *Mol. Pharmacol.* 75 (2009) 525–533.
- [11] A.K. Pathak, M. Bhutani, A.S. Nair, K.S. Ahn, A. Chakraborty, H. Kadara, S. Guha, G. Sethi, B.B. Aggarwal, Ursolic acid inhibits STAT3 activation pathway leading to suppression of proliferation and chemosensitization of human multiple myeloma cells, *Mol. Cancer Res.* 5 (2007) 943–955.
- [12] S.K. Sandur, M.K. Pandey, B. Sung, B.B. Aggarwal, 5-hydroxy-2-methyl-1,4-naphthoquinone, a vitamin K3 analogue, suppresses STAT3 activation pathway through induction of protein tyrosine phosphatase, SHP-1: potential role in chemosensitization, *Mol. Cancer Res.* 8 (2010) 107–118.
- [13] K.S. Ahn, G. Sethi, B. Sung, A. Goel, R. Ralhan, B.B. Aggarwal, Guggulsterone, a farnesoid X receptor antagonist, inhibits constitutive and inducible STAT3 activation through induction of a protein tyrosine phosphatase SHP-1, *Cancer Res.* 68 (2008) 4406–4415.
- [14] B.R. Blechacz, R.L. Smoot, S.F. Bronk, N.W. Werneburg, A.E. Sirica, G.J. Gores, Sorafenib inhibits signal transducer and activator of transcription-3 signaling in cholangiocarcinoma cells by activating the phosphatase shatterproof 2, *Hepatology* 50 (2009) 1861–1870.
- [15] F. Yang, C. Brown, R. Buettner, M. Hedvat, R. Starr, A. Scuto, A. Schroeder, M. Jensen, R. Jove, Sorafenib induces growth arrest and apoptosis of human glioblastoma cells through the dephosphorylation of signal transducers and activators of transcription 3, *Mol. Cancer Ther.* 9 (2010) 953–962.
- [16] P.T. Wan, M.J. Garnett, S.M. Roe, S. Lee, D. Niculescu-Duvaz, V.M. Good, C.M. Jones, C.J. Marshall, C.J. Springer, D. Barford, R. Marais, Mechanism of activation of the RAF-ERK signaling pathway by oncogenic mutations of B-RAF, *Cell* 116 (2004) 855–867.
- [17] A. Noury, A. Zamboni, L. Davies, I. Niculescu-Duvaz, H.P. Dijkstra, D. Menard, C. Gaulon, D. Niculescu-Duvaz, B.M. Suijkerbuijk, F. Friedlos, H.A. Manne, R. Kirk, S. Whittaker, R. Marais, C.J. Springer, BRAF inhibitors based on an imidazo[4,5]pyridin-2-one scaffold and a meta substituted middle ring, *J. Med. Chem.* 53 (2010) 1964–1978.
- [18] F. Gu, Y. Ma, Z. Zhang, J. Zhao, H. Kobayashi, L. Zhang, L. Fu, Expression of Stat3 and Notch1 is associated with cisplatin resistance in head and neck squamous cell carcinoma, *Oncol. Rep.* 23 (2010) 671–676.